Presentation of a Mobile Testing Device for the Inspection of Micropiles of Rockfall Protection Nets in Alpine Terrain

Jörg Edler,[1] Matthias Rebhan,[2] Emanuel Troyer[1]

[1] Graz University of Technology, Faculty of Mechanical Engineering and Economic Sciences, Graz, Austria
joerg.edler@tugraz.at, emanuel.troyer@tugraz.at
[2] Graz University of Technology, Faculty of Civil Engineering Sciences, Graz, Austria
rebhan@tugraz.at

The protection of structural facilities in alpine regions from natural hazards--particularly rockfalls--is becoming increasingly important due to global warming. While installing protection systems such as rockfall nets is an important first step, these systems require long-term maintenance and regular inspection to ensure functionality. Although inspection of the nets themselves is often feasible in alpine terrain, inspection of the ground anchors has not been possible until now. This challenge motivated the development of a hydraulically powered, mobile testing device specifically designed to evaluate the ground anchors of rockfall nets in alpine areas. The hydraulic concept enables the required forces to be generated within a short time, while the compact design allows the device to be carried through difficult terrain by just two people.

DOI
https://doi.org/10.18690/um.fs.7.2025.17

ISBN
978-961-299-049-7

Keywords:
micropile,
testing,
testing device,
Impulse cylinder,
dynamic testing

University of Maribor Press

1 Introduction

Micropiles (ground anchors) have proven to be a reliable foundation element for protective structures, as they are able to transfer impulsive tensile loads resulting from natural hazards such as rockfall into the subsoil. In contrast to conventional foundations, where permanent loads are decisive, protective structures are primarily subjected to dynamic actions [1]. However, standardised procedures to adequately capture the dynamic behaviour of micropiles under realistic loading conditions are still limited.

Previous investigations considered different concepts for energy input, including mechanical and pneumatic approaches. These methods, however, showed considerable practical limitations, which shifted the research focus towards hydraulic solutions. By using hydropneumatic accumulators, hydraulic systems can provide the required impulse efficiently, reproducibly, and in a field-applicable manner. This makes it possible to realistically simulate the characteristic loading of micropiles in protective structures [1], [2].

The present work builds on these developments and explores the application of hydraulic testing systems for dynamic micropile loading. The objective is to highlight the potential of this approach for both research and practice and to provide a basis for the further advancement of dynamic testing methods.

2 State of the art to test micropiles

Micropiles have become a widely used foundation element for protective structures against natural hazards such as rockfall, avalanches or debris flows. In contrast to their application in conventional foundations, where mainly permanent static loads are decisive, micropiles in protective structures are predominantly subjected to short-term, impulsive tensile loads [1]. This fundamental difference requires adapted design and testing methods to ensure reliable performance under dynamic conditions.

2.1 Protective structures and micropile foundations

Protective structures (see Figure 1) are designed to reduce the consequences of natural hazards to an acceptable level, thereby safeguarding infrastructure and settlement areas and ensuring economic sustainability. While earth embankments dissipate impact energy through their mass and internal load transfer, flexible systems such as rockfall protection nets rely on a combination of interception structures, superstructures and cables to redirect forces into the foundation [1]. Micropiles act as key anchorage elements in these systems, transferring high tensile forces into the ground.

Figure 1: Typical projective structures.
Source: [1]

2.2 Characteristics and installation challenges

According to EN 14199 (2016), micropiles are versatile elements used to reduce settlements and transfer compressive or tensile loads. In protective structures, however, their function differs from classical geotechnical applications: tensile loading is often eccentric, and additional deflections arise due to cable extensions and system flexibility [1]. Installation in steep or inaccessible terrain poses further challenges, as lightweight drilling rigs are required and the use of fully cased or double corrosion-protected elements is often restricted. Current developments therefore investigate self-drilling micropiles with double corrosion protection (DCP-SBZ) as a potential solution [2]. Different tendon diameters (DN22–DN40) are

commonly used depending on the load level and boundary conditions of the protective structure.

Conventional testing procedures

As with anchors (EN 1537:2015) or soil nails (EN 14490:2010), micropiles must be tested to validate design assumptions and ensure functionality. Investigation, suitability and acceptance tests are defined depending on the project stage [1]. In Austria, acceptance criteria include the creep rate ($k_s \leq 5$ mm, ONR 24810:2020) as well as conditions regarding constant load maintenance and maximum load decrease.

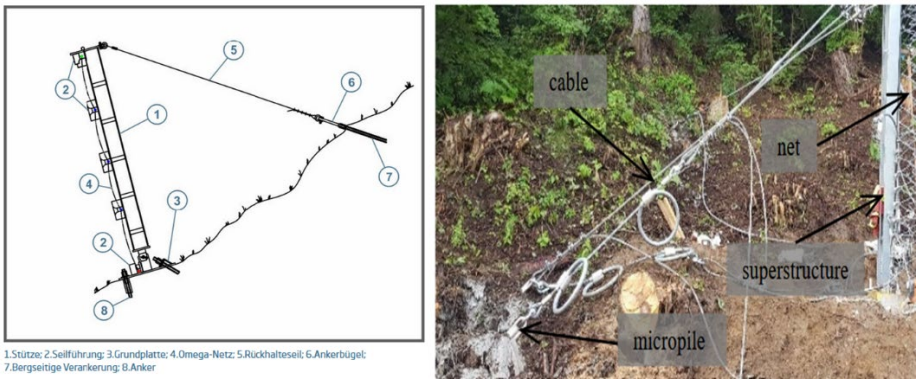

Figure 2: Micropile installation.
Source: Trumer Schutzbauten and [1]

For protective structures, however, the creep-rate criterion appears only of limited relevance, as the actual loading case is defined by short-term impacts. Static testing procedures therefore provide insufficient insight into the real behaviour of micropiles under dynamic conditions [1].

2.3 Approaches to dynamic testing

Dynamic testing methods have so far been mainly applied to large-diameter piles, where wave propagation techniques (e.g. ASTM D5882-16) are used to evaluate production quality and structural integrity. While useful in that context, such methods provide little information on the tensile bearing capacity of micropiles [1], [3]. Drop-weight systems and other commercial testing devices (e.g. Allnamics)

demonstrate the general feasibility of dynamic loading, but their application to small-diameter micropiles in tension remains restricted [1]. Against this background, research efforts have focused on developing dedicated test concepts capable of reproducing the impulsive loading scenarios relevant for protective structures. Pendulum-based approaches, inspired by Charpy impact tests, represent one line of investigation and mark an important step towards the establishment of suitable dynamic test procedures for micropiles [1].

3 Requirements for a new dynamic testing device

The development of a dynamic micropile testing device aims to meet the objectives outlined in the preceding chapters. To achieve this, specific technical and practical requirements must be fulfilled. Table 1 summarises the main criteria, which represent an initial consolidation of conceptual considerations and can be refined in the course of further development.

Table 1: Requirements for a dynamic micropile testing device

Requirement	Description
Dynamic loading	Application of an impulsive load up to 250 kN
Load rise time	The target force must be applied within a maximum of 5 ms to reproduce impact-like loading [1]
Adjustable load level	Impulse should be adjustable on-site between 100 kN and 250 kN
Simple handling	Device should only need to be mounted and pre-tensioned on site
Reaction system	Ideally, no external abutment required; optional integration for higher loads or research purposes
Weight	Device should be portable by two persons, even in rough terrain
Compatibility	Interchangeable adapters to connect to different tendon diameters (DN22 to DN40)

source: own source

4 Construction and function of the dynamic testing device

4.1 General design

The dynamic micropile testing device is based on a hydraulic impulse cylinder, developed at the Institute of Production Engineering, TU Graz. Its design enables the rapid application of tensile impulses up to 250 kN within ≤ 5 ms, fulfilling the

requirements defined in Chapter 3. A CAD model with the main components is shown in Figure 3.

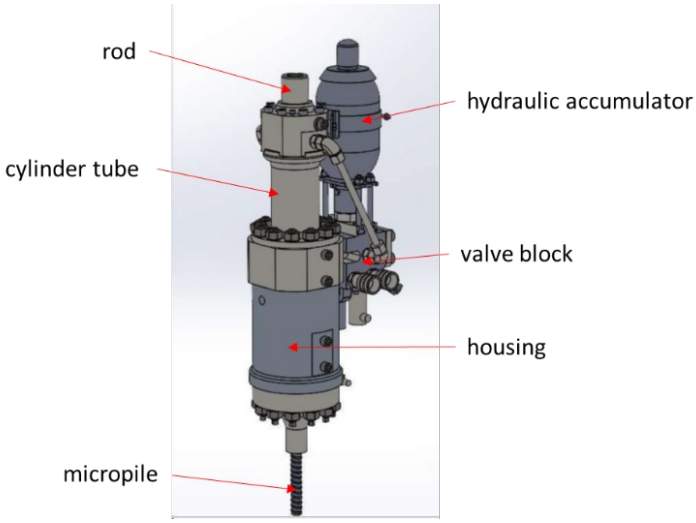

Figure 3: Impulse cylinder.
Source: own source.

4.2 Accumulator system

A bladder-type accumulator is integrated. It separates hydraulic oil and nitrogen by an elastomer bladder; pre-charging stores hydraulic energy that is released when the valve opens, covering peak flow demand and allowing millisecond-scale piston acceleration. The current design allows maximum accumulator charging pressures up to 450 bar, providing sufficient energy for impulsive load levels typical of protective structures [1], [2]. Unlike conventional systems, there is no separate safety shut-off valve on the accumulator; instead, a dedicated hydraulic circuit ensures pressure control and safe energy release.

4.3 Cylinder–piston unit

The piston–cylinder assembly is optimised for very high acceleration. No piston seal is used; sealing to the environment is achieved solely by rod seals. This reduces moving mass and internal friction, enabling the required stroke velocity. The rod

seals face high dynamic loads because sliding speeds reach up to 15 m/s in this application. Under such conditions, frictional heating, lubrication breakdown, and extrusion must be considered. Design guidance from hydraulic fundamentals and sealing handbooks recommends pressure- and temperature-stable materials, optimised lubrication, and anti-extrusion back-up elements; high-performance PU or PTFE composite rod seals are commonly used for piston velocities above ~10 m/s to 15 m/s [10], [11].

4.4 Valve technology

A 2/2 seat-type directional valve is used (rather than a spool valve) for tight shut-off, lower contamination sensitivity, and short actuation travel. In the rest position, a spring keeps the valve closed; when pilot pressure is applied, the valve opens and the accumulator discharges into the cylinder chamber, producing rapid piston acceleration (see Figure 4) [10].

4.5 Impulse generation

When the valve opens, hydraulic fluid acts on the piston surface, accelerating it until it strikes the impact plate at the cylinder head. The resulting momentum transfer generates the impulsive tensile load that is transmitted to the micropile. The stroke is ~130 mm; after impact, oil returns to tank via the return lines, and the piston retracts for the next cycle.

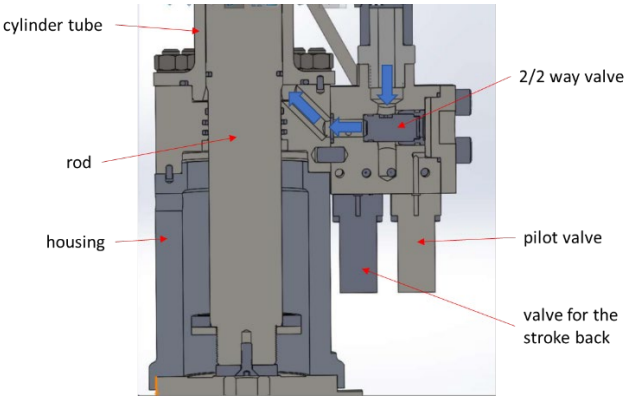

Figure 4: Valve block and oil flow.
Source: own source.

4.6 Hydraulic supply

Lab tests used a compressed-air driven hydraulic pump (up to ~700 bar). For field use, a battery-driven pump unit is foreseen to ensure mobility in alpine terrain.

4.7 Control of impulse intensity

The impulse $\mathbf{p}$ depends on piston mass and velocity:

$$\mathbf{p} = m\,\mathbf{v}, \quad \mathbf{v} = \frac{Q}{A} \tag{1}$$

with Q the flow rate through the valve and A the piston area. Thus, system pressure and valve geometry govern piston velocity and the resulting impulse [4], [10]. This allows on-site adjustment of test loads between 100 kN to 250 kN as specified in Chapter 3 [1].

4.8 End-of-stroke cushioning

At the extremely high rod speeds in this device (up to 25 m/s), uncontrolled end-of-stroke impact would produce harmful pressure spikes, rebound, and structural stress. End-of-stroke cushioning ("cushions") decelerates the piston/rod assembly near the stroke limit by restricting the outflow from the cushioning chamber or by introducing energy-absorbing elements. This converts the kinetic energy $E_k = \frac{1}{2} m_{eq} v^2$ into fluid or material work over a defined cushion travel ΔL, limiting peak force and pressure [12] to [16].

In this application, cushioning not only protects components but also enables the targeted impulse transfer: by braking the piston rod in a controlled manner, the impulse change Δp is shaped so that the required reaction force within ≤ 5 ms is achieved. Thus, the cushioning is directly linked to the fulfilment of the functional requirement defined in Chapter 3.

As a first approach, an elastomeric buffer was implemented. The specially shaped rubber cushion acts as a deformable damping element at the end of the piston stroke. Its geometry was optimized using finite element (FEM) simulations, allowing the

energy absorption characteristics and stiffness profile to be tailored to the impulse requirement. Compared to fluid-based cushions, this solution offers a compact design and robust behaviour under the very short impulse durations considered here. Literature describes various approaches, including plunger/bushing tapers, grooved pistons, and progressive multi-stage metering to control fluid discharge [12] to [15]. For high-energy systems, a combination of material-based buffers (e.g., elastomer pads) with fluid cushioning can provide additional robustness.

5 Calculation of the elastomeric buffer for end-of-stroke cushioning

In order to realise the required end-of-stroke cushioning within ≤5 ms, an elastomeric buffer was designed and analysed. The buffer is intended to absorb the residual kinetic energy of the piston rod after impulse transfer, thereby shaping the impulse change and generating the defined reaction force. Three different buffer geometries were evaluated using finite element method (FEM) simulations, each aiming to achieve a favourable stress distribution, controllable deformation, and reproducible damping behaviour.

Because elastomeric materials exhibit a strongly nonlinear stress–strain relationship even within the elastic regime, all calculations were performed using nonlinear FEM. This approach accounts for large deformations, geometric nonlinearity, and the nonlinear constitutive behaviour of rubber-like materials, ensuring that stiffness and damping effects are represented realistically.

5.1 Variant A – Solid elastomer disc (Shore 40)

The baseline design consisted of a solid rubber disc with a uniform thickness. The material selected was a standard elastomer with Shore A 40, representing a comparatively soft and energy-absorbing configuration. This variant was used as reference to evaluate the achievable stiffness and deformation without additional geometric modifications.

5.2 Variant B – Chamfered disc (Shore 40)

To reduce stress peaks and to create a softer transition during compression, the second variant introduced a chamfer on the inner edge of the same Shore 40 disc. The chamfer modifies the local stiffness and allows the buffer to engage progressively, distributing stresses more evenly across the contact surface. Nonlinear FEM results indicate that the chamfer geometry can delay the onset of maximum stresses and provide a smoother force–displacement response.

5.3 Variant C – Structured disc with cavities (3D-printed, Shore 50)

As a third concept, a 3D-printed elastomer disc with integrated cavities was investigated. The structured geometry was designed to guide deformation into specific zones, reducing stiffness in selected areas while retaining higher strength elsewhere. Due to the limitations of additive manufacturing materials, the available elastomer had a higher hardness (Shore A 50) compared to the previous variants. Despite the higher base stiffness, nonlinear FEM analyses showed that the targeted cavities effectively reduced the effective modulus and enabled controlled energy dissipation.

5.4 Model setup and simulation outputs

Symmetry of the cylinder–buffer assembly was exploited to reduce the computational cost and, in our case, to allocate the freed degrees of freedom to a finer mesh in the region of interest.

The optimized geometry resulting from the nonlinear analysis is a rubber disc with internal holes (see Figure 5). The perforations are designed to guide and localize deformation, thereby tailoring the effective stiffness and energy absorption of the elastomer.

Figure 6 presents the computed force–time response. The initial condition for the simulation is a cylinder-rod velocity of $v_0 = 5$ m/s. The contact force rises rapidly to a peak and then exhibits a damped oscillation. This oscillatory decay is attributed to the combined effects of material/structural damping and contact interaction,

while the rod continues to bear against the hard stop, maintaining a compressive preload during the rebound phase.

Figure 5: 3D printed elastic buffer.
Source: own source.

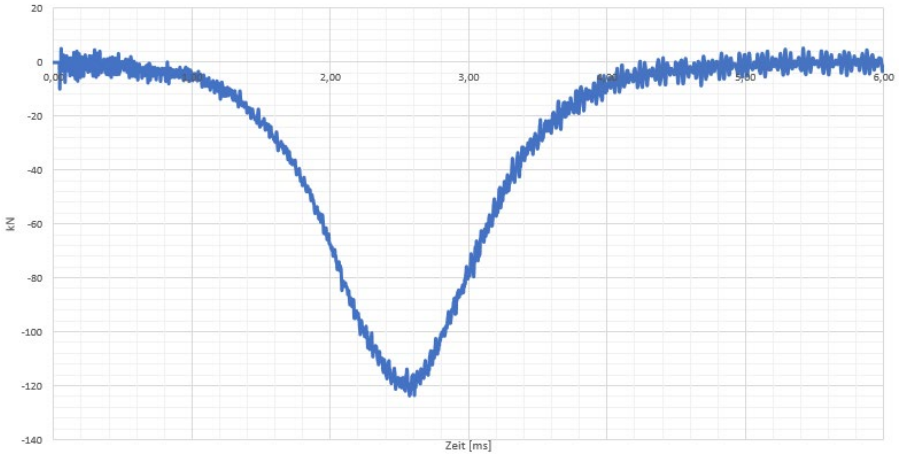

Figure 6: Simulated impact of the cylinder rod into the buffer variant C with 5 m/s.
Source: own source.

6 Test and results

Many different tests were made to determine the response of the impuls cylinder on the structure of an micropile. At the beginning all test were made in a laboratory and to field test were made. To measure the reaction force on the micropile was one of the most challenges. Different methods were investigated:

- High speed camera to determine the speed of the cylinder rod.
- Laser vibrometer to determine the reaction velocity on the housing of the cylinder.
- Load cell to measure the reaction force directly.

The best results came out from the solid joint, which can be seen in Figure 7 left, as data recording system a system from National Instruments was used.

The whole system was mounted on a steel construction with a weight of about 5000 kg (see Figure 7 right). The connection between the structure and the micropile was made as a welding construction, because it has been seen that a screw solution can not be fixed. The connection between the micropile and the impulse cylinder is the original screw of the micropile which must be fixed after each test, resulted by the pitch of the screw on the micropile.

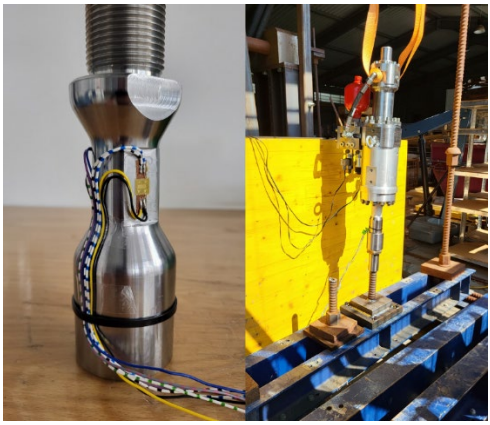

Figure 7: DMS measuring system (left) and mounted impulse cylinder on the test rig (right).
Source: own source.

The tests were made with different pressures in the hydraulic accumulator. The pre pressure of the accumulator is 70 bar so the tests were started with 100 bar up to 250 bar. It was not a hydraulic accumulator with a maximum pressure of 450 bar uses, for the first test a accumulator with a maximum pressure of 300 bar was used.

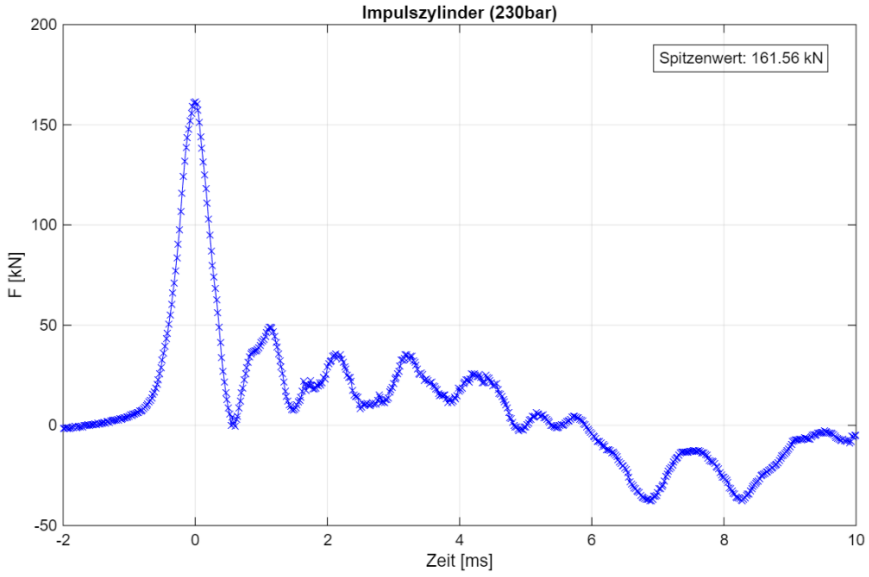

Figure 8: Test of the Impulse Cylinder with 230 bar supply pressure.
Source: own source.

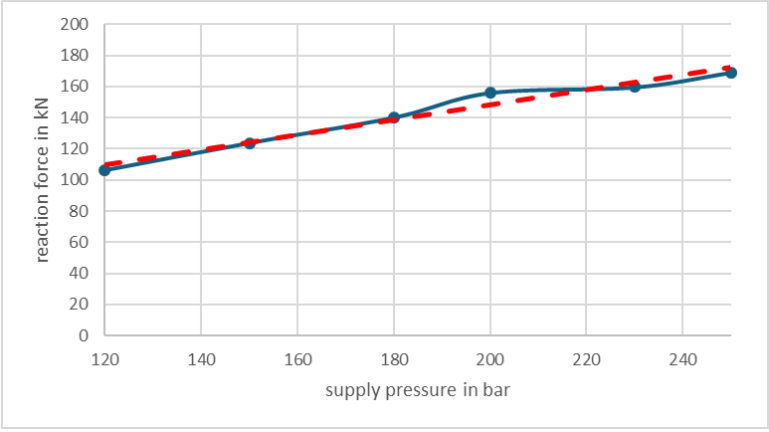

Figure 9: Test series over the supply pressure.
Source: own source.

Figure 8 shows the result of the test with 230 bar. It can be seen that the force rises up in 0.5 ms to a maximum of 161 kN and decrease in 0.5 ms back to zero. Then oscillation can be seen. These oscillation results out of the damping system and of the whole structure of the test rig.

Figure 9 shows all test, a linear dependency between 120 bar and 250 bar of supply pressure can be seen. Pressures under 100 bar cannot be tested resulted by the pre pressure of the hydraulic accumulator.

7 Conclusion

Protective structures in alpine regions increasingly rely on micropiles (ground anchors) to safely transfer impulsive tensile loads from rockfall events into the subsoil. Existing static test procedures do not capture this dynamic loading regime, motivating the development of a mobile, hydraulic impulse device for in-situ verification of micropile performance. Building on state-of-the-art concepts, the device applies adjustable tensile impulses up to 250 kN with a load rise time ≤ 5 ms, while remaining field-portable (two-person carry) and compatible with common tendon sizes (DN22 to DN40). The design features a bladder accumulator (final concept up to 450 bar), a 2/2 seat-type valve for rapid discharge, and a piston–cylinder unit without a piston seal (external tightness via high-speed rod seals).

To shape the impulse and avoid rebound/overloads at high rod speeds (up to 15 m/s), an end-of-stroke cushioning concept was implemented using an elastomeric buffer. Three geometries were assessed via nonlinear FEM: (A) solid Shore-40 disc, (B) Shore-40 disc with inner chamfer for smoother engagement, and (C) structured, additively manufactured disc (Shore-50) with internal cavities for guided deformation. The elastomer behaviour was modelled with a Mooney–Rivlin formulation to reflect geometric and material nonlinearity.

Laboratory and initial field tests investigated multiple measurement strategies (high-speed camera, laser vibrometer, load cell, and a strain-gauged solid joint). The solid-joint approach delivered the most reliable reaction-force data. With a pre-charge of 70 bar and supply pressures from 100 bar to 250 bar (300 bar accumulator used in the first campaign), the device produced fast impulses; e.g., at 230 bar the force increased to ≈ 161 kN in ~0.5 ms and decayed within another ~0.5 ms, with a largely

linear pressure–force trend between ~120 bar and 250 bar. These results demonstrate the technical feasibility of compact, hydraulic dynamic testing for micropiles and provide a validated basis for further optimisation of the cushioning geometry, the measurement chain, and on-site procedures.

References

[1] Rebhan, M., Marte, R., Kainz, F., & Edler, J. (2024, October 2–4). Dynamic testing of micropiles subjected to tensile loads. In *Proceedings of the 5th European Conference on Physical Modelling in Geotechnics (ECPMG 2024)*, Delft, Netherlands: ISSMGE.

[2] Rebhan, M., König, U., Kogelnig, A., & Schuch, M. (2021). Developments and findings in the area of micropiles used for the foundation of protective structures. Journal of Torrent, Avalanche, Landslide and Rock Fall Engineering, 85(187).

[3] Steurer, A., & Adam, D. (2012). Dynamic pile testing in Austria – experiences and results. Geotechnik, 35(1), 38–48.

[4] Wittel, H., Muhs, D., Jannasch, D., & Vossiek, J. (2009). Roloff/Matek Maschinenelemente (20th ed.). Springer, Berlin. https://doi.org/10.1007/978-3-540-70988-5.

[5] EN 14199 (2016). *Execution of geotechnical works – Micropiles.* Austrian Standards International (ASI), Vienna.

[6] EN 1537 (2015). *Execution of geotechnical works – Ground anchors.* Austrian Standards International (ASI), Vienna.

[7] EN 14490 (2010). *Execution of geotechnical works – Soil nailing.* Austrian Standards International (ASI), Vienna.

[8] ONR 24810 (2020). *Technical protection against rockfall – Terms and definitions, effects of actions, design, monitoring and maintenance.* Austrian Standards International (ASI), Vienna.

[9] ASTM International (2016). *Standard Test Method for Low Strain Impact Integrity Testing of Deep Foundations (ASTM D5882-16).* ASTM, West Conshohocken, PA.

[10] Murrenhoff, H. (2011). *Grundlagen der Fluidtechnik – Teil 1: Hydraulik*. Shaker Verlag, Aachen.

[11] Freudenberg Sealing Technologies (2015). *Hydraulic Sealing Guide.* Technical Manual, Weinheim.

[12] Algar, A., Codina, E., Freire, J., & Castilla, R. (2021). Simulation of hydraulic cylinder cushioning using bond-graph and CFD approaches. *Sustainability, 13*(2).

[13] Lai, Q., Liang, L., Li, J., Wu, S., & Liu, J. (2016). Modeling and analysis on cushion characteristics of fast and high-flow-rate hydraulic cylinder. *Mathematical Problems in Engineering*, 2016.

[14] Schwartz, C., De Negri, V. J., & Climaco, J. V. (2005). Modeling and analysis of an auto-adjustable stroke end cushioning device for hydraulic cylinders. *Journal of the Brazilian Society of Mechanical Sciences and Engineering.*

[15] Chen, X., Chen, F., Zhou, J., Li, L., & Zhang, Y. (2015). Cushioning structure optimization of an excavator arm cylinder. *Automation in Construction.*

[16] Hänchen GmbH. (2020). *Endlagendämpfung – Auslegung von Hydraulikzylindern.* Retrieved from https://www.haenchen-hydraulik.de.